

**Ultra-stable phosphoglucose isomerase through immobilization of cellulose-binding module-tagged thermophilic enzyme on low-cost high-capacity cellulosic adsorbent**

**Suwan Myung<sup>1,2</sup>, Xiao-Zhou Zhang<sup>1</sup>, Y.-H. Percival Zhang<sup>1,2,3\*</sup>**

Running title: One-step protein purification and immobilization

<sup>1</sup> Department of Biological Systems Engineering, Virginia Polytechnic Institute and State University, 210-A Seitz Hall, Blacksburg, VA 24061, USA

<sup>2</sup> Institute for Critical Technology and Applied Science (ICTAS), Virginia Polytechnic Institute and State University, Blacksburg, VA 24061, USA

<sup>3</sup> DOE BioEnergy Science Center (BESC), Oak Ridge, TN 37831, USA

\*Corresponding author. Tel: 540-231-7414; Fax: 540-231-7414; Email: [ypzhang@vt.edu](mailto:ypzhang@vt.edu)

## Abstract

One-step enzyme purification and immobilization was developed based on simple adsorption of a family 3 cellulose-binding module (CBM)-tagged protein on the external surface of high-capacity regenerated amorphous cellulose (RAC). An ORF Cthe0217 encoding a putative phosphoglucose isomerase (PGI, EC 5.3.1.9) from a thermophilic bacterium *Clostridium thermocellum* was cloned and the recombinant proteins with or without cellulose-binding module (CBM) were over-expressed in *E. coli*. The  $k_{cat}$  and  $K_m$  of CBM-free PGI at 60 °C were 2765 s<sup>-1</sup> and 2.89 mM, respectively. PGI was stable at a high protein concentration of 0.1 g/L but deactivated rapidly at low concentrations. Immobilized CBM-PGI on RAC (iCBM-PGI) was extremely stable at ~60°C, nearly independent of its mass concentration in bulk solution, because its local concentration on the solid support was constant. iCBM-PGI at a low concentration of 0.001 g/L had a half-life time of 190 h, approximately 80-fold of that of free PGI. Total turn-over number of iCBM-PGI was as high as  $1.1 \times 10^9$  mole of product per mole of enzyme at 60 °C. These results suggest that a combination of low-cost enzyme immobilization and thermoenzyme led to an ultra-stable enzyme building block suitable for cell-free synthetic pathway biotransformation (SyPaB) that can implement complicated biochemical reactions *in vitro*.

**Keywords:** cell-free synthetic biology, cellulose-binding module, enzyme immobilization, phosphoglucose isomerase, protein purification, synthetic pathway biotransformation (SyPaB), thermoenzyme

## Introduction

Biocatalysis mediated by enzymes is becoming more and more acceptable because of the high selectivity and specificity, modest reaction conditions, low energy consumption, and environmentally friendly conditions<sup>1</sup>. But a single enzyme cannot catalyze complicated biochemical reactions, such as complete oxidation of glucose, complete hydrolysis of lignocellulosic biomass, protein synthesis, and so on. Multiple enzymes in one pot and cell-free biotransformation/ biosynthesis mediated by numerous enzymes are gaining more attention<sup>2-5</sup>. Since enzymes cannot duplicate themselves, stabilization of enzymes is vital for economically viable industrial bioprocesses. Enzyme immobilization prolongs life-time of the enzyme and facilitates enzyme/product separation<sup>6,7</sup>.

Synthetic pathway biotransformation (SyPaB) is the implementation of complicated biochemical reactions by employing the *in vitro* assembly of a large number of enzymes and coenzymes<sup>5,8</sup>. For example, nearly 12 moles of dihydrogen have been produced from per glucose equivalent of polysaccharides and water by the non-natural synthetic pathways containing 13-14 enzymes<sup>9,10</sup>, breaking the Thauer limit for anaerobic hydrogen-producing microorganisms<sup>11</sup>. SyPaB would be economically competitive with microbial fermentation for the production of biocommodities only when (i) all of the enzymes in the SyPaB systems have total turn-over number (TTN) values of more than  $10^7$ - $10^8$  mole of product per mole of enzyme, and (ii) low-cost bulk enzyme production and purification are available<sup>5,8,12</sup>.

SyPaB has numerous potential applications, such as the production of hydrogen, alcohols, and polyols from biomass sugars<sup>8,12</sup>, CO<sub>2</sub> utilization<sup>13,14</sup>, sugar battery<sup>5</sup>, and so on.

Therefore, it is vital to develop low-cost enzyme purification and immobilization technologies so that stabilized bulk enzymes would be Lego-like building blocks for SyPaB projects.

26  
27 Cellulose-binding module (CBM), a key component of cellulase, is responsible for  
28 specifically binding to cellulose and increasing the reaction rates of enzymatic cellulose  
29 hydrolysis<sup>15-17</sup>. Several CBMs have been exploited as an affinity tag for the purification  
30 and immobilization of heterologous fusion proteins on cellulosic supports<sup>16, 18-22</sup>. Among  
31 more than 60 families of carbohydrate-binding modules, a family 3 CBM from the  
32 *Clostridium thermocellum* scaffoldin was chosen as a tag because it can tightly bind to both  
33 crystalline and amorphous cellulose<sup>19, 23</sup>. Cellulose is an ideal low-cost support for enzyme  
34 purification and immobilization because it is cheap, inert, stable, biodegradable, and readily  
35 available in different forms. Commercial microcrystalline cellulose (Avicel, cellulose  
36 nanocrystal) has a low binding capacity and more than 80% of its binding surface is internal  
37<sup>23</sup>. In contrast, regenerated amorphous cellulose (RAC) is made from microcrystalline  
38 cellulose through cellulose dissolution in a cellulose solvent followed by cellulose  
39 regeneration in water<sup>24</sup>. RAC has a much higher binding capacity than cellulose  
40 nanocrystal, nano-cellulose fibers (e.g., bacterial microcrystalline cellulose), and cotton fibers  
41<sup>25</sup>. In addition, all the binding capacity of RAC is external. The use of RAC for enzyme  
42 immobilization would bring three potential benefits as compared to Avicel: less cellulose use,  
43 higher volumetric enzyme concentration, and better substrate/product mass transfer.  
44  
45 Phosphoglucose isomerase (PGI, EC 5.3.1.9), a key enzyme in the glycolysis and  
46 glycogenesis pathways, can reversibly convert glucose-6-phosphate (G6P, an aldose  
47 phosphate) to fructose-6-phosphate (F6P, a ketose phosphate)<sup>26</sup>. For hydrogenesis mediated  
48 by SyPaB, PGI is responsible for regenerating glucose-6-phosphate from fructose-6-phosphate.  
49 Utilization of a rapidly expanding library of thermostable enzymes isolated from  
50 extremophiles is increasingly more important for molecular biology R&D and industrial

51 biocatalysis<sup>5, 8, 27</sup>. In this study, we cloned, expressed, and characterized the putative PGI  
52 from a thermophilic bacterium *Clostridium thermocellum*. To prolong the life-time of the *C.*  
53 *thermocellum* PGI and decrease enzyme purification and immobilization costs, one-step  
54 purification and immobilization was developed. A combination of thermoenzyme and  
55 simple immobilization led to an ultra-stable enzyme that can work at elevated temperatures.

56

57

## Materials and Methods

58 **Chemicals and microorganisms.** All chemicals were reagent grade, purchased from Sigma-

59 Aldrich (St. Louis, MO) and Fisher Scientific (Pittsburgh, PA), unless otherwise noted.

60 Avicel PH105, microcrystalline cellulose, was purchased from FMC (Philadelphia, PA).

61 Regenerated amorphous cellulose (RAC) with a high adsorption capacity was made from

62 Avicel through a series of steps – cellulose slurring in water, cellulose dissolution in

63 concentrated phosphoric acid, and cellulose regeneration in water<sup>24</sup>. The *C. thermocellum*

64 ATCC 27405 genomic DNA was purchased from ATCC<sup>28</sup>. *E. coli* BL21 Star (DE3)

65 (Invitrogen, Carlsbad, CA) containing a protein expression plasmid was used for producing

66 the recombinant protein. The Luria-Bertani (LB) medium was used for *E. coli* cell growth

67 and recombinant protein expression supplemented with 100 µg/mL ampicillin. The

68 oligonucleotides were synthesized by Integrated DNA Technologies (Coraville, IA). The

69 liquid glucose reagent containing hexokinase/glucose-6-phosphate dehydrogenase was

70 purchased from Pointe Scientific Inc. (Canton, MI).

71 **Protein expression plasmid construction.** Plasmid pCIP encoding the CBM-intein-PGI

72 (CIP) and plasmid pCP encoding the CBM-PGI (CP) fusion protein were prepared based on

73 plasmids pCIG<sup>19</sup> and the pCG<sup>25</sup>, respectively. The ORF Cthe0217 encoding a putative PGI

74 was amplified by PCR with a pair of primer 5'- CGG CCT CGA GAT GGA AAG AAT AAA

75 ATT TGA C - 3' (XhoI site underlined) and 5'- CTA GCT GCA GTT ACA AAC GCT CTT C

76 -3' (PstI site underlined). After XhoI and PstI digestion of the PCR product and plasmid  
77 pCIG and pCG, the ligated products were transformed to *E. coli* JM109, yielding plasmids  
78 pCIP and pCP. The DNA sequences of pCIP and pCP were validated by sequencing service  
79 from the Virginia Bioinformatics Institute (Blacksburg, VA).

80 **Recombinant protein expression and purification.** Two hundred milliliters of the LB  
81 culture in 1-L Erlenmeyer flasks were incubated with a rotary shaking rate of 250 rpm at 37  
82 °C. After the absorbance ( $A_{600}$ ) reached *ca.* 0.6, the recombinant protein expression was  
83 induced by adding IPTG (0.1 mM, final concentration). The culture was incubated at 18 °C  
84 for 20 h. The cells were harvested by centrifugation at 4 °C, washed twice by 50 mM of  
85 Tris-HCl buffer (pH 7.5), and re-suspended in a 10 mL of 30 mM Tris-HCl buffer (pH 8.5)  
86 containing 0.5 M of NaCl and 1 mM of EDTA. The cell pellets were lysed by Fisher  
87 Scientific Sonic Dismembrator Model 500 (5-s pulse on and off, total 360 s, at 20%  
88 amplitude) in an ice bath. After centrifugation, the fusion protein CBM-intein-PGI or  
89 CBM-PGI was purified through affinity adsorption on RAC, followed by intein cleavage<sup>19</sup> or  
90 ethyl glycol elution method<sup>25</sup>. Two milliliters of 4 g RAC/L was mixed with the 15 mL of  
91 the cell lysate at room temperature for 10 min. After adsorption, the mixture was  
92 centrifuged by 6,000 rpm at 4 °C for 5 min. The pellets were suspended with 20 mL of 50  
93 mM Tris-HCl buffer (pH 8.5) to remove impure proteins, followed by centrifugation. For  
94 purification of PGI from CBM-intein-PGI, the pellet was washed with 20 mL of 50 mM  
95 HEPES buffer (pH 6.5) containing 0.5 M NaCl. After centrifugation, the RAC slurry was  
96 suspended with 5 mL of 50 mM HEPES buffer (pH 6.5) containing 0.5 M NaCl at 40 °C for 9  
97 h. After centrifugation, the cleaved CBM-free PGI was obtained in the supernatant. For  
98 purification of CBM-PGI, the RAC pellets containing the adsorbed CBM-target protein were  
99 suspended in four RAC pellet volumes of 100% ethyl glycol (EG), i.e., the final EG  
100 concentration was ~80% (v/v). After by 10 min incubation at room temperature followed by

101 centrifugation, the purified CBM-PGI was obtained in the supernatant. Ethylene glycol was  
102 removed by dialysis against 50 mM tris-HCl buffer (pH 7.5) including 100 mM NaCl in an  
103 ice bath. The diluted purified protein was re-concentrated by using the Pall ultra-filtration  
104 centrifugal tubes.

105 **PGI activity assay.** Thermophilic PGI activity was measured by using a discontinuous  
106 approach since thermophilic glucose-6-phosphate dehydrogenase was not available. The  
107 initial reaction rates of PGI were measured based on the generation of the product G6P from  
108 the substrate F6P (Eq. 1). G6P was measured by using glucose-6-phosphate dehydrogenase  
109 (G6PDH) in the presence of  $NAD^+$  (Eq. 2). For simplicity, the amount of G6P was  
110 measured by using the Pointe Scientific glucose assay kit (Canton, MI) and the absorbance of  
111 NADH was measured at 340 nm.



114  
115 The PGI activity was measured in a 100 mM HEPES buffer containing 10 mM  $Mg^{2+}$ , 0.5 mM  
116  $Mn^{2+}$ , and 5 mM F6P at 60 or 37 °C. The pre-warmed substrate solution and the PGI  
117 enzyme solution were mixed well and incubated for 5 min at the tested temperature. The  
118 reactions were stopped by boiling for 3 min. One mL of the reaction solution was mixed  
119 with 1.0 mL of the liquid glucose reagent at 37 °C for 3 min. The absorbance was read at  
120 340 nm with a reference of the blank enzyme solution.

121 **Adsorption and one-step purification and immobilization.** The crude cell lysate  
122 containing CBM-PGI and other *E. coli* cellular proteins was mixed with RAC and Avicel at  
123 room temperature for 10 min. After centrifugation at 12,000 rpm for 3 min, the residual  
124 PGI activity in the supernatant was measured as described above. The maximum adsorption

125 capacity of RAC or Avicel ( $A_{\max}$ ) was calculated following the Langmuir isotherm as  
126 described elsewhere<sup>23,25</sup>. For preparation of iCBM-PGI, the cell lysate was mixed with  
127 RAC at a ratio of ~300 mg of CBM-PGI per gram of RAC added. The pellets were washed  
128 twice in 100 mM of HEPES buffer (pH 7.5) followed by centrifugation. The washed pellets  
129 were suspended in the HEPES buffer containing 10 mM  $Mg^{2+}$  and 0.5 mM  $Mn^{2+}$ , being the  
130 iCBM-PGI slurry. The iCBM-PGI activity was measured as described above and the  
131 protein mass concentration was measured by the ninhydrin assay<sup>29</sup>. The leakage of iCBM-  
132 PGI was investigated following the below protocol. The iCBM-PGI slurry was suspended  
133 in 100 mM HEPES buffer (pH 7.5) containing 10 mM  $Mg^{2+}$  and 0.5 mM  $Mn^{2+}$  at 60 °C,  
134 followed by centrifugation at 12,000 rpm for 3 min. After the supernatant was decanted, the  
135 pellets were suspended in the HEPES buffer again. These washing steps were repeated 50  
136 times. Small amounts of the suspended pellets were withdrawn for the PGI activity assay.

137 **Thermostability of PGI and iCBM-PGI.** The thermostability of the purified CBM-PGI  
138 and immobilized CBM-PGI were measured at different concentrations of enzyme (0.1, 0.01,  
139 0.001 g/L) in 100 mM of HEPES buffer (pH 7.5) containing 150 mM of NaCl and 10 mM of  
140  $MgCl_2$  at 60 °C. The residual PGI activity was immediately measured according to the PGI  
141 activity assay as described above.

142 **Other assays.** Mass concentration of soluble protein was measured by the Bio-Rad modified  
143 Bradford protein kit with bovine serum albumin as a standard protein. 10% SDS-PAGE was  
144 performed in the Tris–glycine buffer as described elsewhere<sup>13,28</sup>.

145

146

## Results

### 147 One-step purification and immobilization

148 Most recombinant proteins produced in *E. coli* are usually purified based on their purification  
149 tags and then are immobilized on a solid support, such as silica gel, alginate beads or matrix.



150 One-step purification, covalent immobilization, and additional stabilization of a poly-His-  
151 tagged-galactosidase by using heterofunctional chelate-epoxy sepabeads has been developed  
152 <sup>30</sup>. As compared to costly synthetic solid supports and relatively complicated chemical  
153 reactions for covalent immobilization, we proposed one-step purification and immobilization  
154 of a family 3 cellulose-binding module (CBM)-tagged enzyme on low-cost, biodegradable,  
155 high-capacity regenerated amorphous cellulose (Fig. 1). After recombinant protein  
156 expression and cell lysis, the CBM-tagged target protein can be specifically adsorbed onto  
157 RAC. After centrifugation followed by washing, other *E. coli* soluble proteins were  
158 removed. Finally, the pellets contained the immobilized purified protein on the external  
159 surface of RAC. This immobilization was conducted based on simple adsorption without  
160 chemical covalent bonds because later we found out that the relatively high ionic strength  
161 HEPES buffer did not wash the adsorbed enzyme from the surface of RAC. CBM-oriented  
162 adsorption and immobilization can avoid random enzyme adsorption on the support. Such  
163 random adsorption may greatly decrease the activity of the immobilized enzyme because the  
164 active site of the enzyme may be blocked by the support.

165

166 Conversion of commercial Avicel by a cellulose solvent to RAC can greatly increase binding  
167 capacity by at least 20-fold, i.e., far more enzymes can be immobilized on the same weight  
168 cellulosic support. The adsorption profiles of the CBM-tagged PGI in the whole cell lysate  
169 were examined on RAC and Avicel. Clearly, their adsorptions obeyed the Langmuir  
170 isotherm (Fig. 2). The maximum binding capacity on RAC was as high as 483 mg protein  
171 per gram of RAC, nearly 54 times of that on Avicel (i.e., 8.88 mg per gram of Avicel). High  
172 enzyme immobilization capacity on RAC meant high volumetric enzyme loading. In  
173 addition, the externally-bound enzyme on the surface of RAC may lower mass diffusional  
174 hindrance.

175

176 **Basic characteristics of PGI enzymes**

177 Four different purified forms of PGI enzymes -- free CBM-free PGI, free CBM-PGI, and  
178 immobilized CBM-PGI (iCBM-PGI) on RAC and Avicel -- were obtained in this study.

179 CBM-free PGI was produced by *E. coli* BL21(DE3)/pCIP ; CBM-PGI and immobilized  
180 CBM-PGI were produced by *E. coli* BL21(DE3)/pCP. It was noted that the adsorption of  
181 CBM-tagged enzyme on cellulosic materials is reversible and a fraction of the adsorbed  
182 enzyme can be washed by using ethylene glycol (EG) or low ionic strength buffers <sup>25</sup>.

183 Therefore, free CBM-PGI was purified from immobilized CBM-PGI on RAC by EG washing.

184 The purified CBM-free PGI appeared to be homogenous (Fig. 3, Lane 2). Without EG  
185 elution, immobilized CBM-PGI was obtained after RAC adsorption and washing. The

186 CBM-free PGI was prepared from a fusion protein CBM-intein-PGI (Fig.3, Lane 3).

187 Through simple adsorption and self-cleavage of intein <sup>19</sup>, the purified CBM-free PGI in the  
188 supernatant appeared to be a single band (Fig. 3, Lane 4). The molecular weights of the  
189 CBM-PGI and CBM-free PGI were 67 and 49 kDa, respectively. Approximately 56 mg of  
190 the purified PGI and 70 mg of the purified CBM-PGI were obtained per liter of the culture  
191 with the purification yields of 37.5% and 18.2 %, respectively. It was estimated that  
192 approximately 350 mg of iCBM-PGI per liter the culture was obtained through one-step  
193 purification and adsorption.

194

195 PGI and CBM-PGI activities had the same optimum temperature (60 °C) at pH 7.5. Each  
196 enzyme retained approximately 90 % of its maximum activity at 50 and 70 °C. But only  
197 approximately 40% of each enzyme's optimum activity was exhibited at 30 °C. The  
198 influence of pH on both PGI and CBM-PGI activity was examined in the following buffers:  
199 citric acid (pH 4, 5 and 6), Tris-HCl (pH 6 and 7), HEPES (pH 7 and 8), TAPS (pH 8 and 9),

200 and sodium carbonate (pH 9, 10 and 11) at 60°C. Both enzymes exhibited the same pH  
201 profiles. PGI had the maximum activity at pH 8.0 in the buffers of HEPES and TAPS.  
202 They had approximately 75% and 40% of their maximum activity at pH 7.0 and pH 9.0,  
203 respectively. PGI in Tris-HCl buffer had 30% lower observed activity than that in the HEPE  
204 buffer at pH 7.0.

205

206 The kinetic constants of PGI, CBM-PGI, and iCBM-PGI were examined at 37 and 60 °C  
207 (Table 1). The CBM-PGI showed slightly low  $k_{cat}$  values than PGI and both exhibited  
208 approximately 3-fold  $k_{cat}$  values when the temperature increased from 37 to 60 °C (Table 1).  
209 CBM-PGI had somewhat lower  $K_m$  value ( $1.86 \pm 0.08$  mM) than that of PGI ( $2.89 \pm 0.42$   
210 mM) at 60 °C. The above results suggested that the fusion of CBM-tag on PGI and  
211 immobilization on RAC or Avicel did not change PGI properties greatly.

212

### 213 **Prolonged stability of iCBM-PGI**

214 The half-life time of free PGI at 60°C greatly depended on its mass concentration from 0.1,  
215 0.01 and 0.001 g/L (Fig. 4a). The half-life time of thermo-inactivation was *ca.* 180 h at 0.1  
216 g/L but decreased to only 2.4 h at a low concentration (0.001 g/L). A relatively low mass  
217 concentration of PGI from 0.001-0.01 g/L lose its activity so fast that TTN of free PGI was  
218 far below the threshold value of  $10^{7-8}$  mole of product per mole of enzyme. The  
219 thermostability of CBM-PGI was almost same as purified PGI (data not shown), suggesting  
220 that CBM tag only did not enhance the thermostability of PGI.

221

222 iCBM-PGI exhibited drastically prolonged half-life times of 310 and 190 h at 0.01 g/L and  
223 0.001 g/L as compared to those of free PGI by 6.3- and 80-fold, respectively (Fig. 4b). At a  
224 high concentration of 0.1 g/L, iCBM-PGI only doubled the half-life time to 360 h as

225 compared to free PGI. The half-life times of iCBM-PGI at different protein concentration  
226 were nearly constant because CBM-PGI concentration on the solid support was nearly  
227 constant. The kinetic constants of iCBM-PGI were examined at 37 and 60 °C (Table 1).  
228 The  $k_{cat}$  and  $K_m$  values of iCBM-PGI on RAC were  $2198 \pm 43 \text{ s}^{-1}$  and  $2.43 \pm 0.15 \text{ mM}$ ,  
229 respectively, small changes as compared to free CBM-PGI and iCBM-PGI on Avicel. The  
230 above results suggested that simple adsorption of CBM-tagged PGI greatly prolonged the  
231 enzyme's life-time but retained most of its activity. Since the TTN value can be simply  
232 calculated without running a continuous biocatalytic process according to the equation of  
233  $TTN = k_{cat}/k_d^{31}$ , iCBM-PGI at 0.001 g/L had a TTN value of  $1.1 \times 10^9$  mole of product per  
234 mole of enzyme, where the observed reaction rate was a half of its maximum reaction rate,  
235 i.e.,  $[S] = 1.2 \text{ mM}$ . Such high TTN values for iCBM-PGI are among the most stable  
236 enzymes in the literature, far higher than the critical values of  $10^{7-8}$  for SyPaB<sup>8</sup>.  
237  
238 It is well-known that adsorbed CBM-tagged protein on RAC may be washed out reversibly,  
239 depending on buffer type and ionic strength. For example, high concentration glycerol or  
240 ethyl glycol, low ionic strength buffer or water can partially wash the adsorbed CBM-tagged  
241 proteins<sup>25</sup>. Therefore, the leaking behavior of iCBM-PGI was investigated under its  
242 working condition [100 mM HEPES buffer (pH 7.5) containing 10 mM  $\text{Mg}^{2+}$  and 0.5 mM  
243  $\text{Mn}^{2+}$  at 60 °C] (Fig. 5). It was found that no significant PGI activity was lost after 50  
244 washings, indicating that iCBM-PGI was stable under this relatively high ionic strength  
245 working buffer for a long time. Therefore, it was not necessary to conduct covalent linking  
246 between RAC and CBM-PGI.

## 248 Discussion

249 A simple protein purification and immobilization protocol was developed based on high

250 affinity of CBM-tagged protein on a large binding capacity cellulosic material - RAC. As  
251 compared to other enzyme immobilization supports, cellulosic materials are very attractive  
252 because they are cheap, biodegradable, and abundant<sup>18-20</sup>. The use of RAC rather than  
253 Avicel can increase enzyme binding capacity by 54 fold. As compared to other cellulosic  
254 materials (such as bacterial cellulose), RAC also presents higher accessibility and is much  
255 less costly<sup>23,25</sup>. The use of RAC for enzyme immobilization would bring more advantages:  
256 (i) a reduction in the mass use of cellulosic support, (ii) the potential for increasing enzyme  
257 loading for high-speed biocatalysis, like carrier-free CLEA vs routine carrier-based enzyme  
258 immobilization<sup>32</sup>, and (iii) a potential reduction in mass diffusion hindrance because all  
259 enzymes are immobilized on the external surface of RAC. Given 300 mg of CBM-PGI  
260 adsorbed by per gram of RAC, one kg of enzyme requires 3.3 kg of RAC for immobilization,  
261 resulting in 4.33 kg of iCBM-PGI. Assuming that the crude recombinant PGI production  
262 costs was \$30/kg enzyme and RAC cost was \$2/kg, the production costs of iCBM-PGI can be  
263 estimated to be \$36.6/kg of CBM-PGI or \$8.45/kg of iCBM-PGI.  
264  
265 Simple enzyme adsorption on the support may have no or some damage to enzyme activity,  
266 depending on the orientation between the active sites of the enzyme and support<sup>6</sup>. To  
267 minimize steric hindrance and environmental effects imposed by the surface properties of the  
268 matrices, a proper distance between the surface of the support and the enzyme is preferred for  
269 efficient immobilization of biocatalytic molecules on solid support materials<sup>33,34</sup>.  
270 Sometimes, enzyme adsorbed on an adsorbent was easily leached out from the support  
271 because of weak interaction between enzyme molecule and surface of supports<sup>35</sup> and extra  
272 covalent bonding may be conducted<sup>30</sup>. In this study, CBM can orient the enzyme  
273 adsorption on the surface of RAC (Fig. 1) so that the active sites of the enzymes had enough  
274 distance from RAC and iCBM-PGI had comparable activity to free enzyme (Table 1). It

275 was noted that the high ionic strength working buffer allowed such simple immobilization to  
276 be stable enough even after 50 washings at 60 °C. Therefore, covalent attachment does not  
277 appear to be necessary.

278  
279 The thermostability of free PGI was strongly associated with its concentration (Fig. 4a),  
280 implying that this enzyme is a multimeric protein. The cloned *C. thermocellum* PGI has a  
281 similarity of 85% as compared to *Bacillus stearothermophilus* PGI<sup>36,37</sup>, which is a dimeric  
282 enzyme. In support of it, the binding capacity ratio of iCBM-PGI on RAC/Avicel was 54,  
283 approximately two times than the value of a monomeric protein of thioredoxin-green  
284 fluorescence protein-CBM<sup>23</sup>. After enzymes were immobilized on the surface of RAC,  
285 their stability depended on their local concentration on the solid support rather than their bulk  
286 concentration. When immobilized enzymes were diluted to very low concentrations in a  
287 liquid solution, their local concentration was not changed so that they retained their activity  
288 and stability, nearly independent of its bulk concentration (Fig. 4b).

289  
290 To enhance the overall reaction rate in a complicated biological reaction network, it is often  
291 expected that there is no rate-limiting step controlled by one of several enzymes<sup>38,39</sup>.

292 However, the  $k_{cat}$  values of several enzymes often differ by three or four orders of magnitude  
293<sup>9,10</sup>. When evenly distribution of the rate-controlling theory for each enzyme was  
294 implemented, it meant that it was necessary for these enzymes to have the respective roughly  
295 three or four orders of magnitude difference in mass concentration. For high-activity  
296 enzymes, it was important to increase their half-time, especially at low enzyme concentration  
297 at the same level as those of low-activity enzymes at high mass concentration. Enzyme  
298 immobilization was a good solution to address such challenge because immobilized enzymes  
299 had nearly a constant life time, independent of its mass concentration in the bulk phase.

300

301 In conclusion, one-step simple protein purification and immobilization method was  
302 developed by adsorbing CBM-tagged proteins by using the low-cost ultra-high capacity  
303 adsorbent RAC. As compared to Avicel as a support<sup>16, 22</sup>, iCBM-PGI on RAC decreased  
304 the cellulosic support use based on weight by 54-fold so that high enzyme loadings were  
305 possible, especially important in SyPaB where more than 10 enzymes were used together.  
306 As compared to carrier-free cross-linked enzyme aggregate<sup>32</sup>, iCBM-PGI avoided random  
307 cross linking, which may hurt enzyme activity, and may have better mass transfer because of  
308 mono-layer adsorption of the enzyme on the large surface solid support -- RAC. Different  
309 from the previous thermoenzymes<sup>28, 39, 40</sup>, the free thermophilic PGI was not stable enough in  
310 a free form for SyPaB but simple immobilization enabled it to be far more stable than what  
311 we required. This simple and low-cost protein purification and purification technology  
312 would have broad applications in enzyme-mediated biomanufacturing.

313

314 **Acknowledgments.** This work was supported mainly by the Air Force Office of Scientific  
315 Research and MURI (FA9550-08-1-0145), and partially by DOE Bioenergy Science Center  
316 (BESC), and CALS Biodesign and Bioprocess Center. SW was partially supported by the  
317 ICTAS Scholar Program.

318 **References**

- 319 1. Schmid, A.; Dordick, J. S.; Kiener, A.; Wubbolts, M.; Withold, B., Industrial  
320 biocatalysis today and tomorrow. *Nature* **2000**, 409, 258-268.
- 321 2. Goerke, A. R.; Swartz, J. R., Development of cell-free protein synthesis platforms for  
322 disulfide bonded proteins. *Biotechnol. Bioeng.* **2008**, 99, (2), 351-367.
- 323 3. Wang, Y.; Zhang, Y.-H. P., Cell-free protein synthesis energized by slowly-  
324 metabolized maltodextrin. *BMC Biotechnol.* **2009**, 9, 58.
- 325 4. Bujara, M.; Schümperli, M.; Billerbeck, S.; Heinemann, M.; Panke, S., Exploiting  
326 cell-free systems: Implementation and debugging of a system of biotransformations.  
327 *Biotechnol. Bioeng.* **2010**, 106, (3), 376-389.
- 328 5. Zhang, Y.-H. P., Production of biocommodities and bioelectricity by cell-free  
329 synthetic enzymatic pathway biotransformations: Challenges and opportunities. *Biotechnol.*  
330 *Bioeng.* **2010**, 105, 663-677.
- 331 6. Krajewska, B., Application of chitin- and chitosan-based materials for enzyme  
332 immobilizations: a review. *Enzyme and Microbial Technology* **2004**, 35, (2-3), 126-139.
- 333 7. Jung, G. Y.; Stephanopoulos, G., A functional protein chip for pathway optimization  
334 and *in vitro* metabolic engineering. *Science* **2004**, 304, (5669), 428-431.
- 335 8. Zhang, Y.-H. P.; Sun, J.-B.; Zhong, J.-J., Biofuel production by *in vitro* synthetic  
336 pathway transformation. *Curr. Opin. Biotechnol.* **2010**, 21, 663-669.
- 337 9. Zhang, Y.-H. P.; Evans, B. R.; Mielenz, J. R.; Hopkins, R. C.; Adams, M. W. W.,  
338 High-yield hydrogen production from starch and water by a synthetic enzymatic pathway.  
339 *PLoS One* **2007**, 2, (5), e456.
- 340 10. Ye, X.; Wang, Y.; Hopkins, R. C.; Adams, M. W. W.; Evans, B. R.; Mielenz, J. R.;  
341 Zhang, Y.-H. P., Spontaneous high-yield production of hydrogen from cellulosic materials  
342 and water catalyzed by enzyme cocktails. *ChemSusChem* **2009**, 2, (2), 149-152.
- 343 11. Thauer, R. K.; Kaster, A. K.; Seedorf, H.; Buckel, W.; Hedderich, R., Methanogenic  
344 archaea: ecologically relevant differences in energy conservation. *Nat. Rev. Microbiol.* **2008**,  
345 6, 579-591.
- 346 12. Wang, Y.; Huang, W.; Sathitsuksanoh, N.; Zhu, Z.; Zhang, Y.-H. P.,  
347 Biohydrogenation from biomass sugar mediated by *in vitro* synthetic enzymatic pathways  
348 *Chemistry & Biology* **2011**, Accepted.
- 349 13. Tong, X.; El-Zahab, B.; Zhao, X.; Liu, Y.; Wang, P., Enzymatic synthesis of L-lactic  
350 acid from carbon dioxide and ethanol with an inherent cofactor regeneration cycle.  
351 *Biotechnol. Bioeng.* **2010P**, n/a-n/a.
- 352 14. Zhang, Y.-H. P., Artificial photosynthesis would unify the electricity-carbohydrate-  
353 hydrogen cycle for sustainability. *Nature Precedings* **2010**, 2010.4167.1.
- 354 15. Zhang, Y.-H. P.; Himmel, M.; Mielenz, J. R., Outlook for cellulase improvement:  
355 Screening and selection strategies. *Biotechnol. Adv.* **2006**, 24, (5), 452-481.
- 356 16. Shoseyov, O.; Shani, Z.; Levy, I., Carbohydrate binding modules: biochemical  
357 properties and novel applications. *Microbiol. Mol. Biol. Rev.* **2006**, 70, 283-295.
- 358 17. Boraston, A. B.; Bolam, D. N.; Gilbert, H. J.; Davies, G. J., Carbohydrate-binding  
359 modules: fine-tuning polysaccharide recognition. *Biochem. J.* **2004**, 382, (3), 769-781.
- 360 18. Ong, E.; Gilkes, N. R.; Warren, R. A. J.; Miller, R. C.; Kilburn, D. G., Enzyme  
361 immobilization using the cellulose-binding domain of a *cellulomonas fimi* exoglucanase. *Nat.*  
362 *Biotechnol.* **1989**, 7, (6), 604-607.
- 363 19. Hong, J.; Wang, Y.; Ye X.; Zhang, Y.-H. P., Simple protein purification through  
364 affinity adsorption on regenerated amorphous cellulose followed by intein self-cleavage. *J.*  
365 *Chromatogr. A* **2008**, 1194, (2), 150-154.



- 366 20. Tomme, P.; Boraston, A. B.; McLean, B.; Kormos, J. M.; Creagh, A. L.; Sturch, K.;  
367 Gilkes, N. R.; Haynes, C. A.; Warren, R. A.; Kilburn, D. G., Characterization and affinity  
368 applications of cellulose-binding domains. *J. Chromatogr. B.* **1998**, 715, 283-296.
- 369 21. Chen, H.; Hsieh, Y.-L., Enzyme immobilization on ultrafine cellulose fibers via  
370 poly(acrylic acid) electrolyte grafts. *Biotechnol. Bioeng.* **2005**, 90, (4), 405-413.
- 371 22. Richins, R. D.; Mulchandani, A.; Chen, W., Expression, immobilization, and  
372 enzymatic characterization of cellulose-binding domain-organophosphorus hydrolase fusion  
373 enzymes. *Biotechnol. Bioeng.* **2000**, 69, (6), 591-596.
- 374 23. Hong, J.; Ye, X.; Zhang, Y.-H. P., Quantitative determination of cellulose  
375 accessibility to cellulase based on adsorption of a nonhydrolytic fusion protein containing  
376 CBM and GFP with its applications. *Langmuir* **2007**, 23, (25), 12535-12540.
- 377 24. Zhang, Y.-H. P.; Cui, J.-B.; Lynd, L. R.; Kuang, L. R., A transition from cellulose  
378 swelling to cellulose dissolution by o-phosphoric acid: Evidences from enzymatic hydrolysis  
379 and supramolecular structure. *Biomacromolecules* **2006**, 7, (2), 644-648.
- 380 25. Hong, J.; Ye X; Wang, Y.; Zhang, Y.-H. P., Bioseparation of recombinant cellulose  
381 binding module-protein by affinity adsorption on an ultra-high-capacity cellulosic adsorbent.  
382 *Anal. Chim. Acta* **2008**, 621, 193-199.
- 383 26. Berg, J. M.; Tymoczko, J. L.; Stryer, L., *Biochemistry*. 5th ed.; W.H. Freeman: New  
384 York, 2002; p xxxviii, 894, [76] p.
- 385 27. Adams, M. W. W.; Kelly, R. M., Finding and using hyperthermophilic enzymes.  
386 *Trends Biotechnol.* **1998**, 16, (8), 329-332.
- 387 28. Wang, Y.; Zhang, Y.-H. P., A highly active phosphoglucomutase from *Clostridium*  
388 *thermocellum*: Cloning, purification, characterization, and enhanced thermostability. *J. Appl.*  
389 *Microbiol.* **2010**, 108, 39-46.
- 390 29. Zhu, Z.; Sathitsuksanoh, N.; Zhang, Y.-H. P., Direct quantitative determination of  
391 adsorbed cellulase on lignocellulosic biomass with its application to study cellulase  
392 desorption for potential recycling. *Analyst* **2009**, 134, 2267-2272.
- 393 30. Pessela, B. C. C.; Mateo, C.; Carrascosa, A. V.; Vian, A.; Garcia, J. L.; Rivas, G.;  
394 Alfonso, C.; Guisan, J. M.; Fernandez-Lafuente, R., One-step purification, covalent  
395 immobilization, and additional stabilization of a thermophilic Poly-His-tagged -galactosidase  
396 from *Thermus* sp. strain T2 by using novel heterofunctional chelate-epoxy sephabeads.  
397 *Biomacromolecules* **2003**, 4, (1), 107-113.
- 398 31. Rogers, T. A.; Bommarius, A. S., Utilizing simple biochemical measurements to  
399 predict lifetime output of biocatalysts in continuous isothermal processes. *Chem. Eng. Sc.*  
400 **2010**, 65, (6), 2118-2124.
- 401 32. Cao, L.; Langen, L. v.; Sheldon, R. A., Immobilised enzymes: carrier-bound or  
402 carrier-free? *Curr. Opin. Biotechnol.* **2003**, 14, (4), 387-394.
- 403 33. Deere, J.; De Oliveira, R. F.; Tomaszewski, B.; Millar, S.; Lalaouni, A.; Solares, L.  
404 F.; Flitsch, S. L.; Halling, P. J., Kinetics of Enzyme Attack on Substrates Covalently Attached  
405 to Solid Surfaces: Influence of Spacer Chain Length, Immobilized Substrate Surface  
406 Concentration and Surface Charge. *Langmuir* **2008**, 24, (20), 11762-11769.
- 407 34. Nouaimi, M.; Moschel, K.; Bisswanger, H., Immobilization of trypsin on polyester  
408 fleece via different spacers. *Enzyme and Microbial Technology* **2001**, 29, (8-9), 567-574.
- 409 35. Yiu, H. H. P.; Wright, P. A.; Botting, N. P., Enzyme immobilisation using siliceous  
410 mesoporous molecular sieves. *Microporous and Mesoporous Materials* **2001**, 44, 763-768.
- 411 36. Chou, C. C.; Sun, Y. J.; Meng, M. S.; Hsiao, C. D., The crystal structure of  
412 phosphoglucose isomerase/autocrine motility factor/neuroleukin complexed with its  
413 carbohydrate phosphate inhibitors suggests its substrate/receptor recognition. *J. Biol. Chem.*  
414 **2000**, 275, 23154-23160.

- 415 37. Sun, Y.-J.; Chou, C.-C.; Chen, W.-S.; Wu, R.-T.; Meng, M.; Hsiao, C.-D., The crystal  
416 structure of a multifunctional protein: Phosphoglucose isomerase/autocrine motility  
417 factor/neuroleukin. *Proc. Nat. Acad. Sci. USA* **1999**, 96, (10), 5412-5417.
- 418 38. Stephanopoulos, G. N.; Aristidou, A. A.; Nielsen, J., *Metabolic Engineering:  
419 Principles and Methodologies*. Academic Press: San Diego, 1998.
- 420 39. Myung, S.; Wang, Y. R.; Zhang, Y.-H. P., Fructose-1,6-bisphosphatase from a hyper-  
421 thermophilic bacterium *Thermotoga maritima*: Characterization, metabolite stability and its  
422 implications. *Process Biochem.* **2010**, 45, 1882-1887.
- 423 40. Wang, Y.; Zhang, Y.-H. P., Overexpression and simple purification of the *Thermotoga*  
424 *maritima* 6-phosphogluconate dehydrogenase in *Escherichia coli* and its application for  
425 NADPH regeneration. *Microb. Cell Fact.* **2009**, 8, 30.
- 426

427 **Figure Legends**

428 **Figure 1.** Scheme of one-step purification and immobilization of a CBM-tagged protein on  
429 ultra-large capacity RAC.

430

431 **Figure 2.** The profile of CBM-PGI adsorption on RAC and Avicel at room temperature. The  
432 curves were fitted by the Langmuir equations.

433

434 **Figure 3.** SDS-PAGE analysis of CBM-PGI and PGI purifications. M, marker; lane 1,  
435 soluble CBM-PGI; lane 2, purified CBM-PGI; lane 3, soluble CBM-intein-PGI; lane 4,  
436 purified PGI in the supernatant after its self-cleavage.

437

438 **Figure 4.** Thermo-inactivation profile of different concentration free PGI (a) and  
439 immobilized CBM-PGI (b) in a 100 mM of HEPES buffer (pH 7.5) containing 150 mM NaCl  
440 and 10 mM MgCl<sub>2</sub> at 60 °C.

441

442 **Figure 5.** Leakage of the immobilized CBM-PGI washing in a 100 mM of HEPES buffer (pH  
443 7.5) containing 10 mM Mg<sup>2+</sup> and 0.5 mM Mn<sup>2+</sup>.

444 **Table 1.** The kinetic parameters of PGI and immobilized PGI at different temperatures (pH  
 445 7.5).

		$K_m$ (mM)	$k_{cat}$ (s <sup>-1</sup> )	$k_{cat}/K_m$ (10 <sup>5</sup> s <sup>-1</sup> M <sup>-1</sup> )
PGI	37 °C	1.90 ± 0.24	929 ± 25	4.89
	60 °C	2.89 ± 0.42	2765 ± 335	9.57
CBM-PGI	37 °C	1.02 ± 0.06	729 ± 53	7.15
	60 °C	1.86 ± 0.08	2433 ± 79	13.08
iCBM-PGI	37 °C	2.11 ± 0.14	1091 ± 35	5.17
	60 °C	2.43 ± 0.15	2198 ± 43	9.06
Avicel-CBM-PGI	37 °C	1.53 ± 0.14	946 ± 27	6.18
	60 °C	1.65 ± 0.02	2009 ± 16	12.18

446

447  $K_m$ , Michaelis-Menten constant;  $k_{cat}$ , rate constant

448

Accepted Manuscript

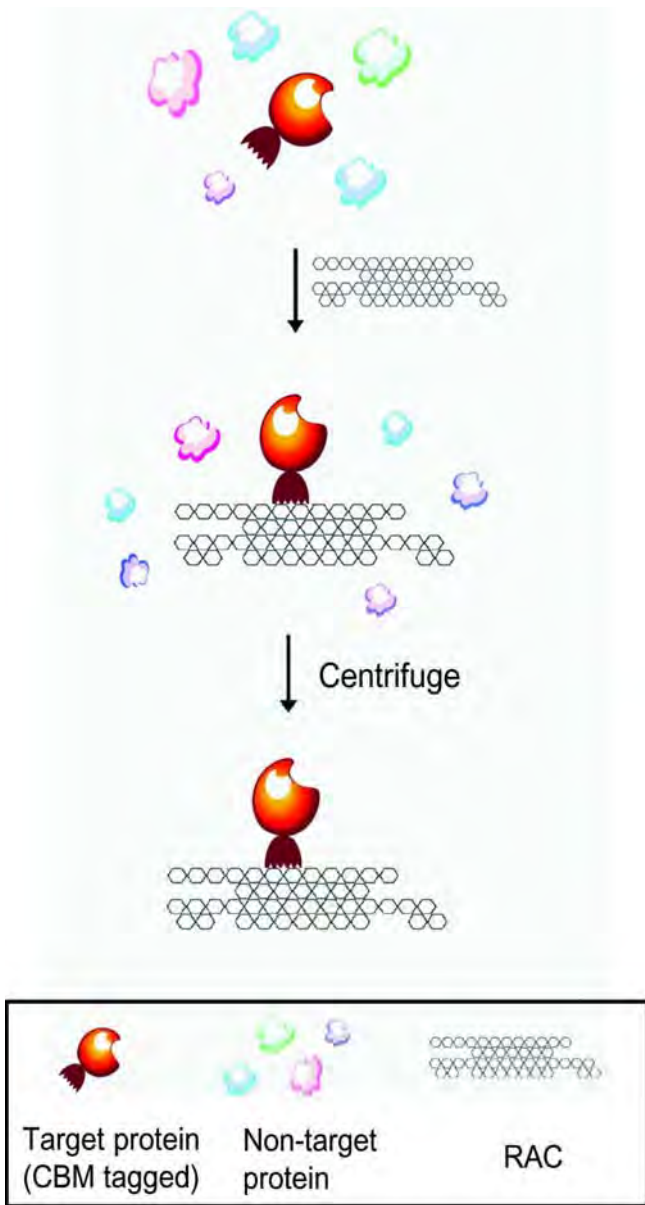


Figure 1  
85x159mm (300 x 300 DPI)

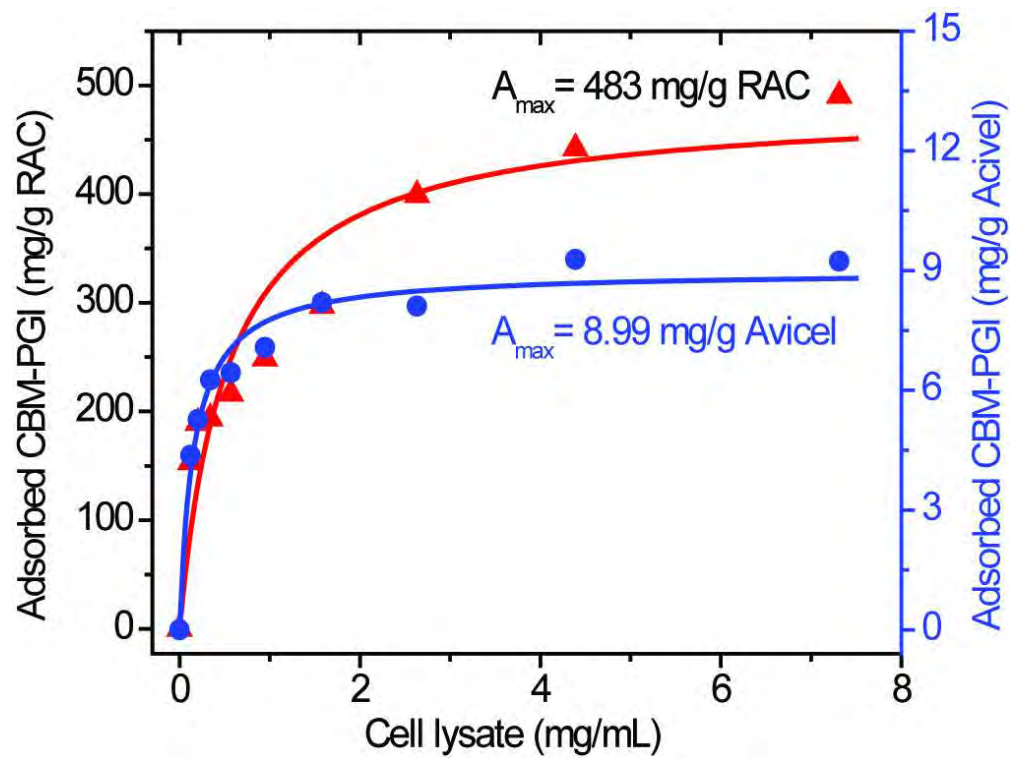


Figure 2  
86x64mm (300 x 300 DPI)

Accepted Article

Accepted Article

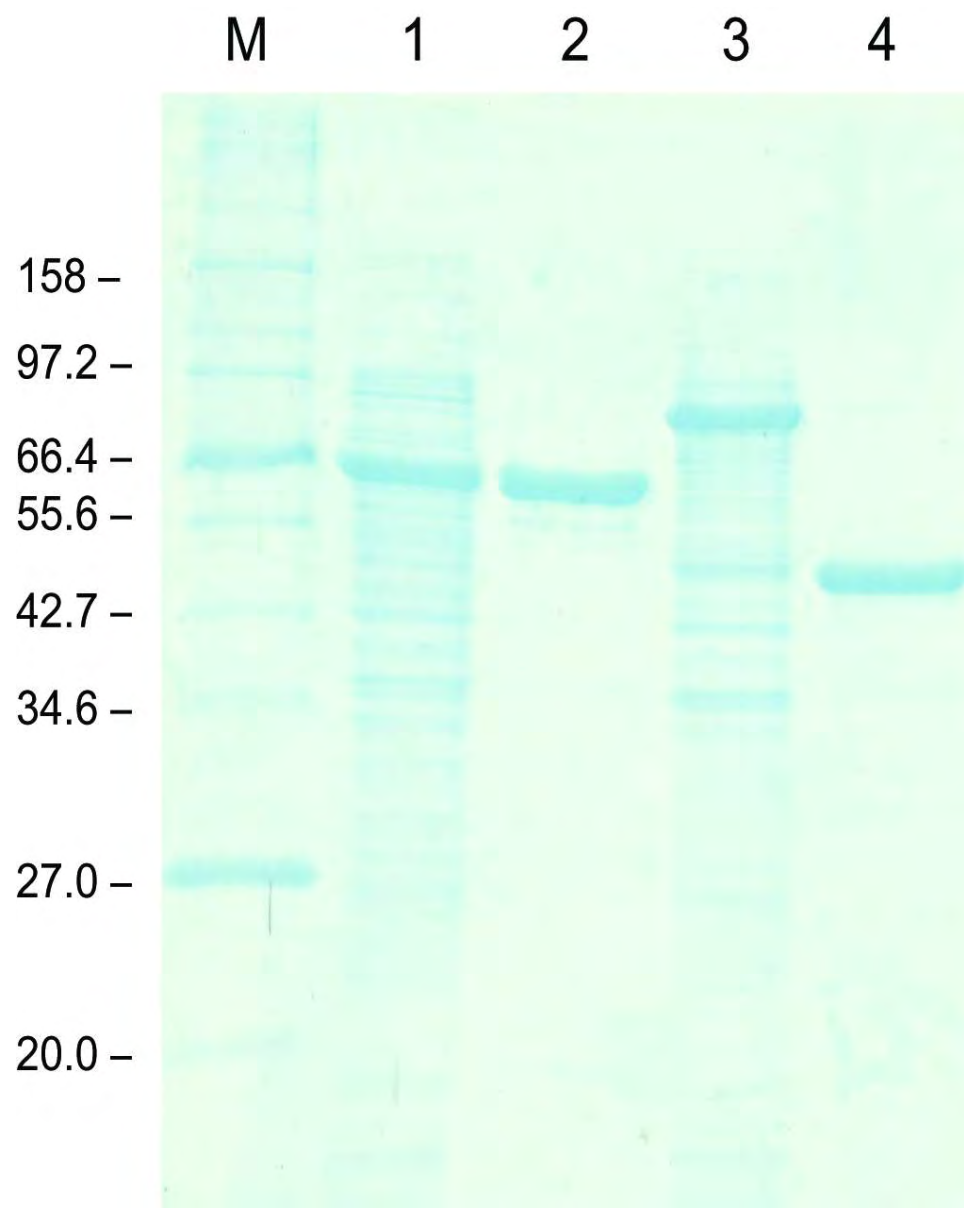


Figure 3  
85x107mm (300 x 300 DPI)

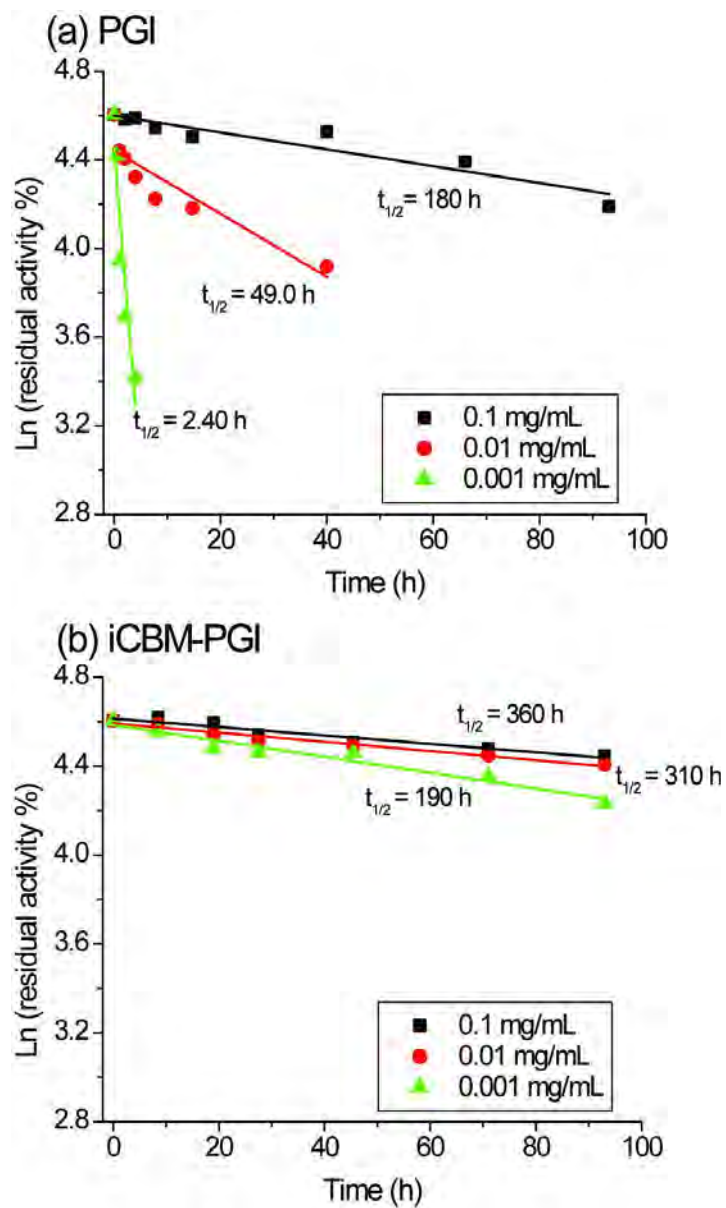


Figure 4  
85x144mm (300 x 300 DPI)



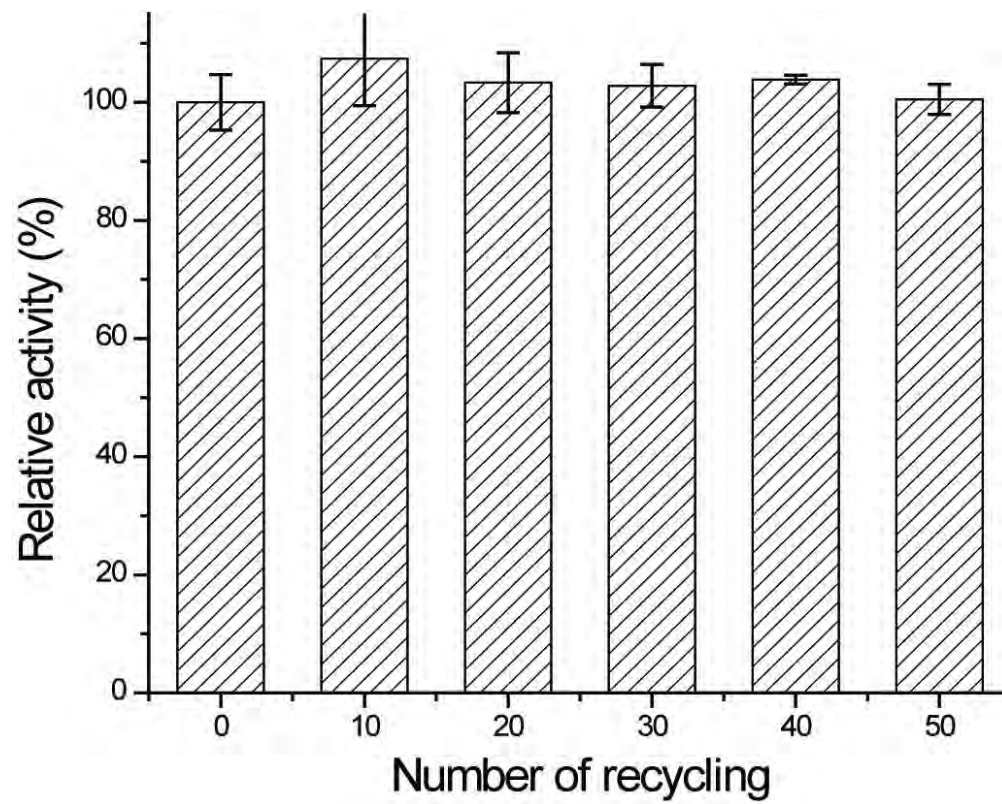


Figure 5  
87x69mm (300 x 300 DPI)

Accept